


## Suppression of Unitary Three-Body Loss in a Degenerate Bose-Fermi Mixture

Xing-Yan Chen<sup>1,2,\*</sup> Marcel Duda<sup>1,2,\*</sup> Andreas Schindewolf<sup>1,2</sup> Roman Bause<sup>1,2</sup>  
Immanuel Bloch,<sup>1,2,3</sup> and Xin-Yu Luo<sup>1,2,†</sup>

<sup>1</sup>Max-Planck-Institut für Quantenoptik, 85748 Garching, Germany

<sup>2</sup>Munich Center for Quantum Science and Technology, 80799 München, Germany

<sup>3</sup>Fakultät für Physik, Ludwig-Maximilians-Universität, 80799 München, Germany

 (Received 4 October 2021; revised 17 March 2022; accepted 22 March 2022; published 14 April 2022)

We study three-body loss in an ultracold mixture of a thermal Bose gas and a degenerate Fermi gas. We find that at unitarity, where the interspecies scattering length diverges, the usual inverse-square temperature scaling of the three-body loss found in nondegenerate systems is strongly modified and reduced with the increasing degeneracy of the Fermi gas. While the reduction of loss is qualitatively explained within the few-body scattering framework, a remaining suppression provides evidence for the long-range Ruderman-Kittel-Kasuya-Yosida (RKKY) interactions mediated by fermions between bosons. Our model based on RKKY interactions quantitatively reproduces the data without free parameters, and predicts one order of magnitude reduction of the three-body loss coefficient in the deeply Fermi-degenerate regime.

DOI: [10.1103/PhysRevLett.128.153401](https://doi.org/10.1103/PhysRevLett.128.153401)

Ultracold mixtures of bosonic and fermionic atoms provide a powerful platform to explore the physics of Bose-Fermi mixtures. Degenerate mixtures have been produced to investigate phase separation [1], superfluidity [2], polarons [3–5], and fermion-mediated interactions [6,7]. Although various phases have been predicted for strongly interacting mixtures, ranging from supersolid charge density wave states [8,9] to boson-mediated  $s/p$ -wave fermion pairing [10–12], experimental investigation is hindered by the strong three-body recombination loss between the atoms [13–16]. Characterizing and understanding the three-body loss is a crucial step toward exploring many-body physics in strongly interacting Bose-Fermi mixtures.

Three-body loss describes the process in which two atoms form a dimer while interacting with a third atom. The released binding energy of the dimer leads to the scattering products escaping the trap [17] and to heating [18]. A formalism for three-body loss in nondegenerate mixtures has been developed [19,20] and confirmed experimentally [15,21,22]. In the universal regime, where the  $s$ -wave scattering length  $a$  is much shorter than the de Broglie wavelength, the three-body loss coefficient  $L_3$  is proportional to  $a^4$ , and can be altered by a series of Efimov

resonances arising from couplings to Efimov-trimer bound states. In the unitary regime, where the scattering length is larger than the de Broglie wavelength, the three-body loss coefficient saturates with  $L_3 \propto 1/T^2$  [20], which has been confirmed experimentally in nondegenerate systems [17,22].

In the quantum degenerate regime, the three-body loss rate strongly depends on quantum statistics and other many-body effects such as the fermion-mediated interactions [6,7,23]. While the three-body recombinations involving identical particles are enhanced (suppressed) by bunching (antibunching) due to Bose [24–26] (Fermi [27,28]) statistics, it remains unexplored how Fermi statistics modifies three-body recombination processes that involve only one fermion. Moreover, the effective boson-boson interaction mediated by the degenerate Fermi gas further complicates the problem. Through the Ruderman-Kittel-Kasuya-Yosida (RKKY) mechanism, two bosons obtain an effective long-range interaction by exchanging one fermion [29]. The RKKY interaction modifies the scattering potential, and thus, the three-body loss rate. The RKKY interaction is predicted to form the basis for several new quantum phases [23,30], however, so far only mean-field effects of this interaction have been observed [6,7].

In this Letter, we study three-body loss in a mixture of thermal  $^{23}\text{Na}$  and Fermi-degenerate  $^{40}\text{K}$ , where we explore the effects of both Fermi statistics and the RKKY interaction. We measure the three-body loss coefficient  $L_3$  at different interspecies scattering lengths. We find that the loss is described by the zero-range theory in the universal regime, while it is reduced by Fermi degeneracy in the unitary regime. In addition to the  $1/T^2$  scaling, the unitary three-body loss decreases with  $T/T_F$  of the Fermi gas

---

Published by the American Physical Society under the terms of the [Creative Commons Attribution 4.0 International](https://creativecommons.org/licenses/by/4.0/) license. Further distribution of this work must maintain attribution to the author(s) and the published article's title, journal citation, and DOI. Open access publication funded by the Max Planck Society.

where  $T_F$  is the Fermi temperature. A theoretical model based on few-body scattering theory, including contributions from the Fermi statistics and the RKKY interaction, quantitatively described the data without any free parameters. Based on this model, more than one order of magnitude reduction in  $L_3$  can be achieved with  $T/T_F < 0.13$ .

The reduction of three-body loss is qualitatively explained by the few-body scattering theory. In the unitary regime, instead of the divergent scattering length, the de Broglie wavelength determines the scattering properties. The unitary three-body loss coefficient for scattering between two identical bosons of mass  $m_b$  and one fermion with mass  $m_f$  is then given by

$$l_3(E) = \frac{8\pi^2 \hbar^4 \cos^3 \phi}{m_r^3 E^2} (1 - e^{-4\eta}), \quad (1)$$

where  $E$  is the kinetic energy in the three-body center-of-mass frame [20,31]. Here,  $m_r = m_b m_f / (m_b + m_f)$  is the reduced mass, and  $\phi$  is defined by  $\sin \phi = m_f / (m_b + m_f)$ . The term  $1 - e^{-4\eta}$ , where  $\eta$  is the inelasticity parameter, gives the probability that the incoming wave is not reflected. The average loss coefficient in an atomic mixture is obtained by averaging over the collision energy distributions  $f(E)$  [32],

$$L_3 = \int l_3(E) f(E) dE. \quad (2)$$

For a nondegenerate mixture, the average collision energy is given by  $3k_B T$ , thus  $L_3 \propto 1/T^2$  in the unitary regime according to Eq. (1). For a mixture where the Fermi gas is degenerate, the average collision energy furthermore depends on the Fermi energy. Because of Fermi statistics, identical fermions distribute over higher momentum states than for the case of a Boltzmann distribution, leading to a larger collision energy as illustrated in Fig. 1. Accordingly, the average unitary three-body loss decreases as the Fermi energy increases. In other words, the saturation of kinetic energy in the Fermi degenerate regime leads to a reduction of three-body loss compared to thermal gases. To explicitly show the effect of Fermi degeneracy, we separate the  $1/T^2$  dependence by defining the temperature-independent loss coefficient  $\Lambda \equiv L_3 T^2$ . In essence, one expects  $\Lambda$  to stay constant in the nondegenerate regime and to decrease with  $T/T_F$  in the Fermi-degenerate regime.

Our experimental sequence begins with the preparation of a trapped mixture of bosonic  $^{23}\text{Na}$  atoms in  $|F, m_F\rangle = |1, 1\rangle$  and fermionic  $^{40}\text{K}$  atoms in  $|9/2, -9/2\rangle$ . Here,  $F$  is the total angular momentum and  $m_F$  is its  $z$  component. The trapping frequencies for Na and K in the  $(x, y, z)$  direction are  $2\pi \times (88, 141, 357)$  Hz and  $2\pi \times (97, 164, 410)$  Hz, respectively. The interspecies scattering length is varied by tuning the magnetic field around a Feshbach resonance at 78.30(4) G [32]. The relation between the scattering length and the

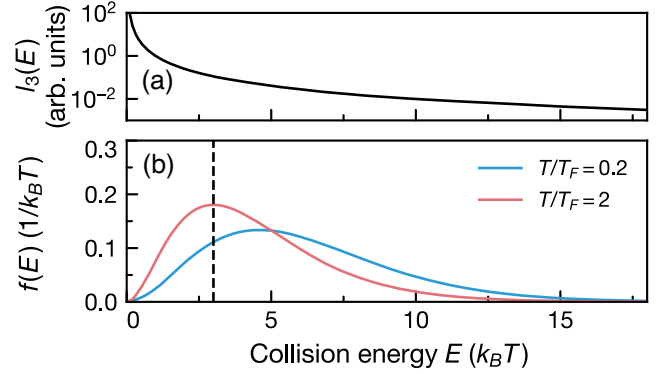


FIG. 1. Three-body loss coefficient and collisional energy distribution. (a) Unitary three-body loss coefficient  $l_3(E) \propto 1/E^2$ , as given by Eq. (1). (b) The distribution function  $f(E)$  of collisional energy in a Bose-Fermi mixture. We show two scenarios with the same temperature  $T$  but different  $T_F$ . For a thermal mixture (red solid line), the distribution follows the six-dimensional Boltzmann distribution with an average collision energy of  $3k_B T$  (black dashed line). For a mixture with a degenerate Fermi gas (blue solid line), the distribution is shifted toward larger collision energies by the Fermi pressure.

magnetic field is obtained by fitting the binding-energy data of the Feshbach molecules, as described in detail in Supplemental Material [32]. To probe the loss on the repulsive (attractive) side of the Feshbach resonance, we prepare the sample at a weakly repulsive interaction below (above) the resonance and ramp the magnetic field in about  $100 \mu\text{s}$  to the target magnetic field. Before the ramp, a magnetic field gradient is turned on to compensate gravitational sag between the atomic species and ensure good density overlap. After a variable hold time, the magnetic field is ramped back within  $100 \mu\text{s}$  to a zero crossing of the interspecies scattering length close the initial magnetic field. Subsequently, the atoms are released from the trap and both species are imaged after some time of flight. We obtain the temperatures and atom numbers from the images and deduce  $T_F$  from the atom number and trapping frequencies.

To characterize the few-body aspect of the three-body loss in our system, we measure  $L_3$  at various scattering lengths. We use  $3 \times 10^5$  Na atoms and  $1.5 \times 10^5$  K atoms. The temperature is chosen to be around  $0.6T_F$  but above the condensation temperature of Na. The measured atom loss ratio between Na and K is close to 2:1, confirming that Na-Na-K is the dominant loss channel, while the K-K-Na three-body loss is suppressed by Pauli blocking between K atoms. We determine  $L_3$  by fitting the loss rates of Na and K atoms to the coupled differential equations

$$\frac{dN_K}{dt} = \frac{1}{2} \frac{dN_{\text{Na}}}{dt} = -L_3 \int n_{\text{Na}}^2(\mathbf{x}) n_{\text{K}}(\mathbf{x}) d^3\mathbf{x}. \quad (3)$$

We use a thermal distribution for  $n_{\text{Na}}(\mathbf{x})$  and a Thomas-Fermi distribution for  $n_{\text{K}}(\mathbf{x})$ . Besides the three-body loss term, we include secondary processes and evaporation in

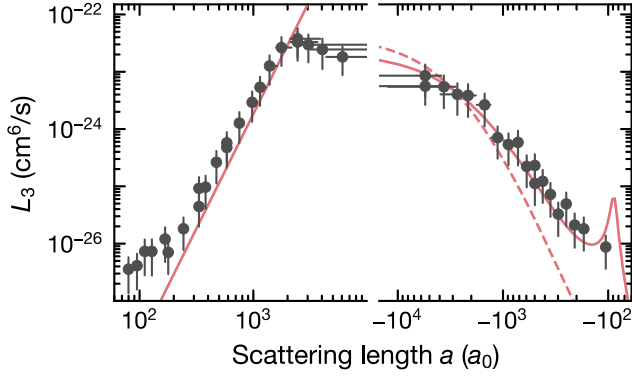


FIG. 2. Three-body loss coefficient  $L_3$  versus interspecies scattering length  $a$  (gray points). The red solid line shows the numerical result of the fitted zero-range theory, which yields an inelasticity parameter  $\eta = 0.02$  and a three-body parameter  $R_0 = 35a_0$  (see Supplemental Material [32]). The red dashed line shows the result with  $\eta = 0.02$  but without Efimov resonances. The error bars are discussed in Supplemental Material [32].

the universal regime [32]. In the unitary regime, these processes become insignificant.

Figure 2 summarizes the results of the three-body loss coefficient  $L_3$  as a function of the interspecies scattering length  $a$ . We compare our results to the zero-range theory, which assumes contact interactions [19,20,32]. The zero-range theory including finite temperature effects requires averaging over the collision energy distribution, and is not available in an analytic form for  $a > 0$ . Therefore, we use the zero-temperature formula for  $a > 0$  [19] and the finite-temperature formula for  $a < 0$  [20]. We find that  $\eta \approx 0.02$  and the three-body parameter  $R_0 = 35a_0$  [32] reproduce the loss in the universal regime on both sides of the resonance. In the short range where the scattering length is comparable to the van der Waals length  $R_{\text{vdW}} = 53.3a_0$ , the zero-range approximation breaks down [43–45] and the theory fails to describe the data.

With a good understanding of the three-body loss in the universal regime, we move on to probe the unitary three-body loss as a function of temperature and Fermi degeneracy. We use the same experimental sequence as in the previous measurements and fix the probe magnetic field to the pole of the Feshbach resonance  $|1/a| \lesssim 10^{-4}a_0^{-1}$  [32]. We vary  $T/T_F$  by changing the initial number of K atoms and the temperature while keeping the mixture in thermal equilibrium. In order to achieve the lowest possible  $T/T_F$ , we use a high number of K atoms ( $\sim 4 \times 10^5$ ) and a low number of Na atoms ( $\sim 3 \times 10^4$ ). Thus, the loss fraction of K atoms is small compared to the loss fraction of Na atoms and  $T/T_F$  is modified by less than 10% throughout a loss measurement. In the high- $T/T_F$  regime, we reduce the number of K atoms down to  $\sim 2 \times 10^4$ . Since a dependence of the three-body loss on  $T/T_F$  is not expected in this regime, we allow for a relative large increase of  $T/T_F$  of about 30%. The initial temperatures and the trap parameters

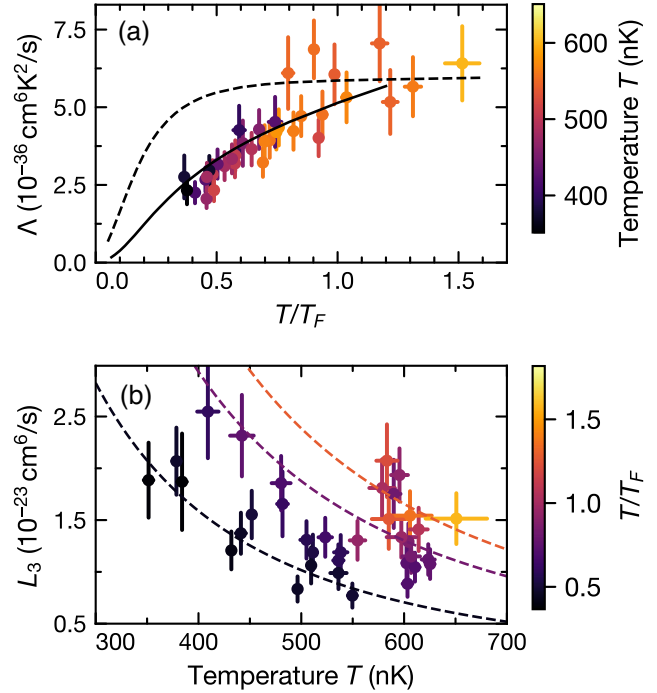


FIG. 3. Suppression of unitary three-body loss. (a) Temperature-independent loss coefficient  $\Lambda$  as a function of  $T/T_F$ . The temperature of each loss measurement is indicated by the color of the data points. The dashed line represents the few-body prediction of  $\Lambda$  according to Eq. (4). The solid line shows the prediction including the RKKY effect. (b) Three-body loss coefficient as a function of temperature. The  $T/T_F$  of the Fermi gas is indicated by the color. The dashed lines show the temperature dependence of  $L_3 = \Lambda/T^2$  for different  $T/T_F$ . The  $\Lambda$  coefficients are obtained by averaging over the data where  $T/T_F$  deviate less than 15% from  $T/T_F = 0.4$  (black), 0.8 (purple), 1.2 (orange). The error bars are discussed in Supplemental Material [32].

are chosen such that temperature changes and evaporation are negligible.

The unitary three-body loss is plotted in Fig. 3. As shown in Fig. 3(a), the temperature-independent loss coefficient  $\Lambda$  is consistent with a saturation for  $T/T_F \gtrsim 1$  and decreases with  $T/T_F$ . A reduction of  $T/T_F$  down to 0.4 leads to a reduction of  $\Lambda$  by a factor 2.4(4) in comparison to the nondegenerate regime. In order to verify that the reduction does not result from a reduced absolute temperature, the measurements in the same  $T/T_F$  regime are taken with different temperatures and atom numbers. As shown in Fig. 3(b), the data for a given  $T/T_F$  follow the inverse-square temperature scaling, while the data for a given temperature  $L_3$  decrease with increasing  $T_F$  for low  $T/T_F$ .

We compare the data with the prediction from the zero-range theory. We use the local density approximation, which treats the mixture at each spatial coordinate in the trap as a homogeneous gas with temperature  $T$  and fugacity  $z$ . The averaged  $\Lambda$  over the three-body density overlap is given by

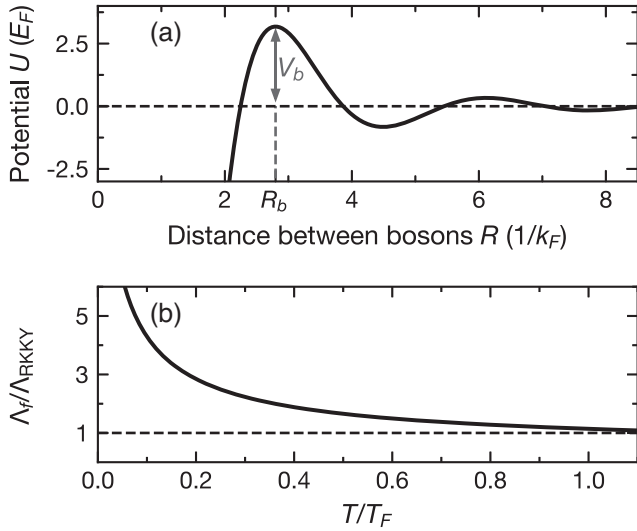


FIG. 4. The effect of the RKKY interactions. (a) RKKY potential mediated by fermions between two bosons at unitarity [32]. The potential barrier  $V_b$  suppresses the tunneling probability into short range. (b) The suppression factor from the RKKY interactions  $\Lambda_f/\Lambda_{\text{RKKY}}$  as a function of  $T/T_F$ .

$$\Lambda_f(T/T_F) = \frac{\int n_{\text{Na}}^2(\mathbf{x})n_{\text{K}}(\mathbf{x})\lambda[z(\mathbf{x})]d^3\mathbf{x}}{\int n_{\text{Na}}^2(\mathbf{x})n_{\text{K}}(\mathbf{x})d^3\mathbf{x}}, \quad (4)$$

where the subscript  $f$  refers to few-body theory. Here,  $z(\mathbf{x})$  is the fugacity under local density approximation,  $\lambda(z) = L_3(z)T^2$  is the local reduced loss coefficient where  $L_3(z)$  is given by Eq. (2) in the degenerate regime and is a function of the local fugacity. The increased collision energy by the Fermi pressure leads to a continuous decrease of  $\Lambda_f$  in the degenerate regime. While the model shows a similar qualitative dependence as the experiment, the experiment data exhibit a substantially larger reduction: the few-body theory suggests significant reduction only for  $T/T_F$  less than 0.1 while the experimental results already show a reduction for  $T/T_F \lesssim 1$ .

In the following, we show that the fermion-mediated RKKY interactions between bosons are crucial to understanding the suppression of the unitary three-body loss. As shown in Fig. 4(a), the RKKY interaction is attractive at short distance and is oscillatory with a length scale  $\pi/k_F$  at long range. At a distance  $R_b = 2.8/k_F$ , the oscillation gives rise to a barrier of the height  $V_b \approx 3.2E_F \propto T_F$  [32]. When the average distance between bosons is much shorter than  $R_b$ , only the short-range attractive interaction played a role [6,7]. In our experiment, the bosons are still thermal with an average distance  $\gtrsim 0.6 \mu\text{m}$  larger than  $R_b \approx 0.3 \mu\text{m}$ . Therefore, the barrier reduces the probability of two bosons approaching each other. In the low-temperature regime, the tunneling probability through the potential barrier  $P_T$  is given by the Bethe-Wigner threshold law  $\sqrt{E/V_b} \propto \sqrt{T/T_F}$  [46], which gives rise to the additional suppression

in the degenerate regime. Again, we apply the local density approximation to obtain the local tunneling probability  $P_T[z(\mathbf{x})] = \sqrt{3k_B T/2V_b[z(\mathbf{x})]}$  from the potential barrier  $V_b[z(\mathbf{x})]$  and the average kinetic energy of the bosons  $3k_B T/2$ . Accordingly, the coefficient  $\Lambda$  is given by

$$\Lambda_{\text{RKKY}}(T/T_F) = \frac{\int n_{\text{Na}}^2(\mathbf{x})n_{\text{K}}(\mathbf{x})\lambda[z(\mathbf{x})]P_T[z(\mathbf{x})]d^3\mathbf{x}}{\int n_{\text{Na}}^2(\mathbf{x})n_{\text{K}}(\mathbf{x})d^3\mathbf{x}}. \quad (5)$$

Equation (5) reproduces the experimental data in the Fermi-degenerate regime without any fitting parameters, as shown in Fig. 3(a). In the deeply degenerate regime, the model predicts more than one order of magnitude reduction, i.e.,  $\Lambda_{\text{RKKY}}(T/T_F < 0.13) < 0.1\Lambda_{\text{th}}$ , where  $\Lambda_{\text{th}}$  is the reduced loss coefficient in a nondegenerate thermal mixture. The suppression from the RKKY effect can be quantified as  $\Lambda_f/\Lambda_{\text{RKKY}}$ , i.e., by comparing to the prediction from the few-body theory. As shown in Fig. 4(b), the suppression factor increase with the Fermi degeneracy. At  $T/T_F = 0.13$ , where we predict reduction of  $\Lambda$  by one order of magnitude compare to  $\Lambda_{\text{th}}$ , the few-body theory predicts a factor of 2.6 reduction, and the RKKY effect suppresses the loss further by a factor of  $\Lambda_f/\Lambda_{\text{RKKY}} \approx 3.7$ . As  $T/T_F$  increases, the form of the mediated interaction breaks down due to thermal fluctuations. Therefore we expect a crossover from the prediction with the mediated interactions in the Fermi-degenerate regime to the constant loss in the thermal regime.

Our model provides a good starting point for further theoretical investigation. Future works could improve the calculation by treating the interaction by nonperturbative methods [47], and by employing the three-body hyperspherical potential [48,49] to go beyond the Born-Oppenheimer approximation used to derive the mediated interaction.

In conclusion, we have investigated the three-body loss of a Bose-Fermi mixture of  $^{23}\text{Na}$  and  $^{40}\text{K}$  both in the thermal and in the Fermi-degenerate regime. We have confirmed that  $L_3$  is proportional to  $a^4$  in the universal regime, and is consistent with saturation at unitarity. We have shown that unitary three-body loss is reduced by the Fermi degeneracy, by measuring the temperature-independent loss coefficient  $\Lambda$  as a function of  $T/T_F$ . While the qualitative feature of the reduction is captured by the few-body scattering theory with the degenerate energy distribution, the additional suppression provides strong evidence for the RKKY effect. We have developed a theoretical model based on RKKY interactions, which quantitatively explains the suppression in the degenerate regime without any fitting parameters. Our model predicts a factor of 10 reduction of  $\Lambda$  for  $0.13T_F$ , a very substantial factor that could be reached in a deeply degenerate mixture.

The understanding of three-body loss rates in the quantum degenerate regime presented in this work provides a promising outlook to investigate strongly interacting

Bose-Fermi mixtures in the deeply degenerate regime. Exciting future works include measuring the unitary collisional loss between a BEC and a degenerate Fermi gas, investigating the universality of unitary Bose-Fermi mixtures [50], probing the Efimov states in the presence of a Fermi sea [49,51,52], understanding the phase transition from atoms to molecules across the unitary regime [53–55], and using three-body loss as a tool to probe three-particle correlation functions [26]. Our work is also relevant for creating degenerate fermionic molecules from Bose-Fermi mixtures by adiabatically tuning the interaction across the unitary regime [56,57], where the suppression of three-body loss could improve the molecule creation efficiency.

We thank E. Tiemann for providing the coupled-channel calculation of Feshbach molecule binding energy, and D. S. Petrov for providing the theory for atom-dimer loss coefficient and discussion about Efimov resonances. We thank B. Huang, R. Schmidt, and A. Christianen for stimulating discussions. We gratefully acknowledge support from the Max Planck Society, the European Union (PASQuanS Grant No. 817482) and the Deutsche Forschungsgemeinschaft under Germany’s Excellence Strategy–EXC-2111–390814868 and under Grant No. FOR 2247. A. S. acknowledges funding from the Max Planck Harvard Research Center for Quantum Optics.

\*These two authors contributed equally.

†xinyu.luo@mpg.de

- [1] R. S. Lous, I. Fritsche, M. Jag, F. Lehmann, E. Kirilov, B. Huang, and R. Grimm, *Phys. Rev. Lett.* **120**, 243403 (2018).
- [2] I. Ferrier-Barbut, M. Delehaye, S. Laurent, A. T. Grier, M. Pierce, B. S. Rem, F. Chevy, and C. Salomon, *Science* **345**, 1035 (2014).
- [3] M.-G. Hu, M. J. Van de Graaff, D. Kedar, J. P. Corson, E. A. Cornell, and D. S. Jin, *Phys. Rev. Lett.* **117**, 055301 (2016).
- [4] Z. Z. Yan, Y. Ni, C. Robens, and M. W. Zwierlein, *Science* **368**, 190 (2020).
- [5] I. Fritsche, C. Baroni, E. Dobler, E. Kirilov, B. Huang, R. Grimm, G. M. Bruun, and P. Massignan, *Phys. Rev. A* **103**, 053314 (2021).
- [6] B. J. DeSalvo, K. Patel, G. Cai, and C. Chin, *Nature (London)* **568**, 61 (2019).
- [7] H. Edri, B. Raz, N. Matzliah, N. Davidson, and R. Ozeri, *Phys. Rev. Lett.* **124**, 163401 (2020).
- [8] I. A. Shelykh, T. Taylor, and A. V. Kavokin, *Phys. Rev. Lett.* **105**, 140402 (2010).
- [9] O. Cotlet, S. Zeytinoglu, M. Sigrist, E. Demler, and A. Imamoglu, *Phys. Rev. B* **93**, 054510 (2016).
- [10] T. Enss and W. Zwerger, *Eur. Phys. J. B* **68**, 383 (2009).
- [11] F. P. Laussy, A. V. Kavokin, and I. A. Shelykh, *Phys. Rev. Lett.* **104**, 106402 (2010).
- [12] J. J. Kinnunen, Z. Wu, and G. M. Bruun, *Phys. Rev. Lett.* **121**, 253402 (2018).
- [13] S. Ospelkaus, C. Ospelkaus, L. Humbert, K. Sengstock, and K. Bongs, *Phys. Rev. Lett.* **97**, 120403 (2006).
- [14] K. Günter, T. Stöferle, H. Moritz, M. Köhl, and T. Esslinger, *Phys. Rev. Lett.* **96**, 180402 (2006).
- [15] R. S. Bloom, M. G. Hu, T. D. Cumby, and D. S. Jin, *Phys. Rev. Lett.* **111**, 105301 (2013).
- [16] S. Laurent, M. Pierce, M. Delehaye, T. Yefsah, F. Chevy, and C. Salomon, *Phys. Rev. Lett.* **118**, 103403 (2017).
- [17] U. Eismann, L. Khaykovich, S. Laurent, I. Ferrier-Barbut, B. S. Rem, A. T. Grier, M. Delehaye, F. Chevy, C. Salomon, L. C. Ha, and C. Chin, *Phys. Rev. X* **6**, 021025 (2016).
- [18] T. Weber, J. Herbig, M. Mark, H.-C. Nägerl, and R. Grimm, *Phys. Rev. Lett.* **91**, 123201 (2003).
- [19] K. Helfrich, H.-W. Hammer, and D. S. Petrov, *Phys. Rev. A* **81**, 042715 (2010).
- [20] D. S. Petrov and F. Werner, *Phys. Rev. A* **92**, 022704 (2015).
- [21] L. J. Wacker, N. B. Jørgensen, D. Birkmose, N. Winter, M. Mikkelsen, J. Sherson, N. Zinner, and J. J. Arlt, *Phys. Rev. Lett.* **117**, 163201 (2016).
- [22] J. Ulmanis, S. Häfner, R. Pires, F. Werner, D. S. Petrov, E. D. Kuhnle, and M. Weidemüller, *Phys. Rev. A* **93**, 022707 (2016).
- [23] S. De and I. B. Spielman, *Appl. Phys. B* **114**, 527 (2014).
- [24] E. A. Burt, R. W. Ghrist, C. J. Myatt, M. J. Holland, E. A. Cornell, and C. E. Wieman, *Phys. Rev. Lett.* **79**, 337 (1997).
- [25] J. Söding, D. Guéry-Odelin, P. Desbiolles, F. Chevy, H. Inamori, and J. Dalibard, *Appl. Phys. B* **69**, 257 (1999).
- [26] E. Haller, M. Rabie, M. J. Mark, J. G. Danzl, R. Hart, K. Lauber, G. Pupillo, and H.-C. Nägerl, *Phys. Rev. Lett.* **107**, 230404 (2011).
- [27] T. B. Ottenstein, T. Lompe, M. Kohnen, A. N. Wenz, and S. Jochim, *Phys. Rev. Lett.* **101**, 203202 (2008).
- [28] J. H. Huckans, J. R. Williams, E. L. Hazlett, R. W. Stites, and K. M. O’Hara, *Phys. Rev. Lett.* **102**, 165302 (2009).
- [29] M. A. Ruderman and C. Kittel, *Phys. Rev.* **96**, 99 (1954).
- [30] H. P. Büchler and G. Blatter, *Phys. Rev. Lett.* **91**, 130404 (2003).
- [31] C. H. Greene, B. Esry, and H. Suno, *Nucl. Phys. A* **737**, 119 (2004).
- [32] See Supplemental Material at <http://link.aps.org/supplemental/10.1103/PhysRevLett.128.153401> for the characterization of the Feshbach resonance, details on the evaporation, secondary loss and secondary heating during three-body recombination, theory predictions for the three-body recombination and three-body recombination with Fermi degeneracy, which includes Refs. [23,33–42].
- [33] T. G. Tiecke, Properties of potassium, available online at <http://www.tobiastiecke.nl/archive/PotassiumProperties.pdf> (2011).
- [34] C. Klempt, T. Henninger, O. Topic, M. Scherer, L. Kattner, E. Tiemann, W. Ertmer, and J. J. Arlt, *Phys. Rev. A* **78**, 061602(R) (2008).
- [35] C. Chin and P. S. Julienne, *Phys. Rev. A* **71**, 012713 (2005).
- [36] A. Viel and A. Simoni, *Phys. Rev. A* **93**, 042701 (2016).
- [37] A. D. Lange, K. Pilch, A. Prantner, F. Ferlaino, B. Engeser, H.-C. Nägerl, R. Grimm, and C. Chin, *Phys. Rev. A* **79**, 013622 (2009).
- [38] E. Tiemann (private communication).
- [39] O. J. Luiten, M. W. Reynolds, and J. T. M. Walraven, *Phys. Rev. A* **53**, 381 (1996).

- [40] A. Mosk, S. Kraft, M. Mudrich, K. Singer, W. Wohlleben, R. Grimm, and M. Weidemüller, *Appl. Phys. B* **73**, 791 (2001).
- [41] D. S. Petrov (private communication).
- [42] B. Huang, K. M. O'Hara, R. Grimm, J. M. Hutson, and D. S. Petrov, *Phys. Rev. A* **90**, 043636 (2014).
- [43] Y. Wang and P. S. Julienne, *Nat. Phys.* **10**, 768 (2014).
- [44] C. Langmack, R. Schmidt, and W. Zwerger, *Phys. Rev. A* **97**, 033623 (2018).
- [45] A. Pricoupenko and D. S. Petrov, *Phys. Rev. A* **100**, 042707 (2019).
- [46] G. Quéméner, [arXiv:1703.09174](https://arxiv.org/abs/1703.09174).
- [47] Y. Nishida, *Phys. Rev. A* **79**, 013629 (2009).
- [48] J. P. D'Incao, H. Suno, and B. D. Esry, *Phys. Rev. Lett.* **93**, 123201 (2004).
- [49] D. J. MacNeill and F. Zhou, *Phys. Rev. Lett.* **106**, 145301 (2011).
- [50] T.-L. Ho, *Phys. Rev. Lett.* **92**, 090402 (2004).
- [51] N. G. Nygaard and N. T. Zinner, *New J. Phys.* **16**, 023026 (2014).
- [52] F. F. Bellotti, T. Frederico, M. T. Yamashita, D. V. Fedorov, A. S. Jensen, and N. T. Zinner, *New J. Phys.* **18**, 043023 (2016).
- [53] D. C. E. Bortolotti, A. V. Avdeenkov, and J. L. Bohn, *Phys. Rev. A* **78**, 063612 (2008).
- [54] G. Bertaina, E. Fratini, S. Giorgini, and P. Pieri, *Phys. Rev. Lett.* **110**, 115303 (2013).
- [55] A. Guidini, G. Bertaina, D. E. Galli, and P. Pieri, *Phys. Rev. A* **91**, 023603 (2015).
- [56] L. D. Marco, G. Valtolina, K. Matsuda, W. G. Tobias, J. P. Covey, and J. Ye, *Science* **363**, 853 (2019).
- [57] M. Duda, X.-Y. Chen, A. Schindewolf, R. Bause, J. von Milczewski, R. Schmidt, I. Bloch, and X.-Y. Luo, [arXiv:2111.04301](https://arxiv.org/abs/2111.04301).